# Possible Steering flows from SAR-derived surface wind asymmetry over loop track of Typhoon Saola (2023)

Guosheng Zhang[1], Pak Wai Chan[2], and Hui Su[3]

[1]Nanjing University of Information Science and Technology
[2]Hong Kong Observatory
[3]Hong Kong University of Science and Technology

September 05, 2024

**Abstract**

Typhoon Saola's (2023) anti-clockwise loop track was monitored by six spaceborne synthetic aperture radar (SAR) images, offering a unique opportunity to investigate the physical factor known as steering flow, a widely accepted concept for studying tropical cyclone (TC) movement and storm surges. Despite its importance, direct observations of steering flows are limited. To address the complex movements observed during the loop track, we propose a novel method to decompose the SAR-derived high-resolution surface wind field into: 1) symmetric rotational winds, 2) general steering flow across three consecutive SAR cases within ˜24 hours, and 3) the remaining steering flow. Our analysis reveals that the newly determined remaining steering flows from north effectively explain the loop track associated with two general steering flows, identified as the western North Pacific summer monsoon (WNPSM) from southeast and Indian summer monsoon (ISM) from southwest.

**Hosted file**

`GRL_Manuscript_SAR_Steering_flow_V3.2.docx` available at https://authorea.com/users/828465/articles/1222696-possible-steering-flows-from-sar-derived-surface-wind-asymmetry-over-loop-track-of-typhoon-saola-2023

**Hosted file**

`SupplementV3.2.docx` available at https://authorea.com/users/828465/articles/1222696-possible-steering-flows-from-sar-derived-surface-wind-asymmetry-over-loop-track-of-typhoon-saola-2023

# Possible Steering flows from SAR-derived surface wind asymmetry over loop track of Typhoon Saola (2023)

**Guosheng Zhang[1,2*], Pakwai Chan[3], and Hui Su[4]**

[1]School of Marine Sciences, Nanjing University of Information Science and Technology, Nanjing 210044, China

[2]Key Laboratory of Meteorological Disaster, Ministry of Education & Collaborative Innovation Center on Forecast and Evaluation of Meteorological Disasters, Nanjing University of Information Science and Technology, Nanjing 210044, China

[3]Hong Kong Observatory, Kowloon, Hong Kong, China

[4]Department of Civil and Environmental Engineering, The Hong Kong University of Science and Technology, Clear Water Bay, Hong Kong, China

*Corresponding author: Guosheng Zhang (zhanggs@nuist.edu.cn)

**Key Points:**

- Six cases of surface wind fields over a loop track made by Typhoon Saola (2023) have been observed by synthetic aperture radar (SAR)
- An innovative method is proposed to derive a physic factor for tropical cyclone movement, known as steering flow from SAR-wind asymmetry
- Summer monsoons from south and new steering flows from north are detected by our new method which effectively explain the loop track

## Abstract

Typhoon Saola's (2023) anti-clockwise loop track was monitored by six spaceborne synthetic aperture radar (SAR) images, offering a unique opportunity to investigate the physical factor known as steering flow, a widely accepted concept for studying tropical cyclone (TC) movement and storm surges. Despite its importance, direct observations of steering flows are limited. To address the complex movements observed during the loop track, we propose a novel method to decompose the SAR-derived high-resolution surface wind field into: 1) symmetric rotational winds, 2) general steering flow across three consecutive SAR cases within ~24 hours, and 3) the remaining steering flow. Our analysis reveals that the newly determined remaining steering flows from north effectively explain the loop track associated with two general steering flows, identified as the western North Pacific summer monsoon (WNPSM) from southeast and Indian summer monsoon (ISM) from southwest.



## Plain Language Summary

The factors what make typhoon/hurricane moving from one place to another have been studied for decades, but direct observations of these factors for tropical cyclone (TC) movement have been limited. Here we design an original approach to identify large-scale flows crucial for steering TC vortex from their footprint on the surface wind asymmetry, focusing on explaining the loop track of Typhoon Saola (2023). Given the complex movements during the loop track, we decompose the surface wind asymmetry into a general steering flow over three consecutive cases within ~24 hours, along with the residual steering flow for each case. Our findings indicate that new steering flows, identified using synthetic aperture radar (SAR) observations, originate from the northeast and northwest, interacting with summer monsoons (also derived from SAR data), and effectively explain the TC's movement.

## 1 Introduction

Understanding tropical cyclone (TC) movements is essential for improving forecasts and reducing the associated damages (e.g. Chu et al., 2012; Kossin, 2018; Hassanzadeh, 2020; Wang & Toumi, 2021). And steering flow is a concept for TC movement studies based on ideal assumptions of a rotating cylinder TC vortex and a unified steering flow surrounding the vortex. Although they are simple, the steering flow can explain many TC movement features (Chan and Gray, 1982; Chan, 2005) and have been widely used for TC movement studies (e.g. Chu et al., 2012; Kossin, 2018; Wang & Toumi, 2021). During storm surge modeling, this concept is adopted and denoted as a unified background wind field for the TC surface wind reconstruction (e.g. Lin and Chavas, 2012; Marsooli et al., 2019). The unified background wind vector is supposed to be linearly related to TC movements. However, the steering flow as a crucial physic feature for TC movement has not been well monitored.

As the spaceborne synthetic aperture radar (SAR) advantages of high spatial resolution and sea surface wind directly retrieval, it is suitable for the steering flow and TC movement investigations. Until now, SAR-derived surface wind field has been widely used for traditional TC measurements of intensity, radius of maximum wind (RMW), size of R34, R50 and R64 (e.g. Zhang et al., 2017; Reul et al., 2017; Howell et al., 2022). However, TC movement, as the most important factor to induce asymmetric surface wind structure (Klotz & Jiang, 2016; Zhang et al., 2021), has not been well studied. Recently, the unified background wind vector (or steering flow) has been extracted from SAR-derived wind field and can explain most TC asymmetric surface wind structures (Zhang et al., 2021).

Typhoon Saola (2023) made an interesting anti-clockwise loop track. Generally, there are two summer monsoon systems in August (Fig. A1) influencing the vortex movement there: 1) the western North Pacific summer monsoon (WNPSM) and 2) the Indian summer monsoon (ISM) (Ding & Chan, 2005; Xiang et al., 2013; He et al., 2024). If no new steering flows exsiting, the loop track cannot be made. Consequently, there would be more steering flows surrounding the loop track of Typhoon Saola (2023) than steering flows of summer monsoons. Taking the SAR advantage of high spatial resolution, we propose a new approach to examine the possibility of two steering flows and their potential to explain the interesting vortex movements in the loop track. In this study, two sets of three continuous SAR-wind fields in about 24 hours provide a unique opportunity to determine the complicated steering flows: 1) general steering flow over three cases synchronously and 2) the respective steering flow for each case by removing the general steering flow. The remainder of this paper is organized as follows: six SAR-derived surface wind fields and the method proposed in this study are in section 2. The results of steering flows and investigations of the vortex movement over the loop track are in Section 3. Finally, conclusions are given in Section 4.

## 2 Data and Method

### 2.1 SAR Observations of surface wind fields

Typhoon Saola (2023) exhibited a looping track from August 25 to 28. To explore the steering flows during this movement, we obtained six SAR images and generated 2D sea surface

wind maps. These six wind field cases, linked to Saola's 'anti-clockwise loop' track, are shown in Fig. 1.

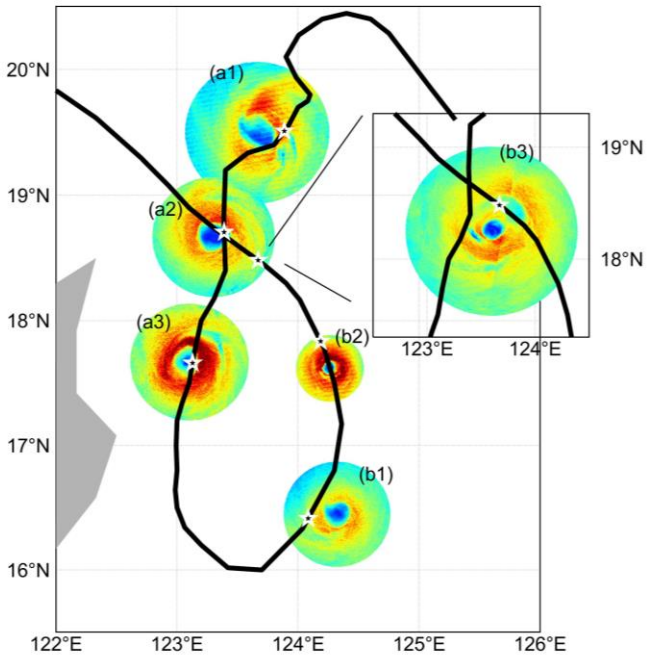


Fig. 1. Six SAR-derived wind fields of $r < 3R_{max}$ over Typhoon Saola (2023) related to the loop track acquired at: (a1) 09:53 UTC on August 25, (a2) 21:46 UTC on August 25, (a3) 10:00 UTC on August 26, (b1) 21:31 UTC on August 27, (b2) 09:44 UTC on August 28, and (b3) 21:37 UTC on August 28. The first five are from RADARSAT Constellation Mission (RCM) and the last one is from Sentinel-1A.

The SAR-derived wind field has a spatial resolution of approximately 500 meters. The first set of three cases (Fig. 1a1 to Fig. 1a3) occurred within about 24 hours from August 25 09:53 UTC to August 26 10:00 UTC, with intervals of roughly 12 hours each. Similarly, the second set of three cases (Fig. 1b1 to Fig. 1b3) also took place within approximately 24 hours from August 27 21:31 UTC to August 28 21:37 UTC, with similar intervals. The left set of images (Fig. 1a) captures the TC's structure as it forms the 'anti-clockwise loop,' while the right (Fig. 1b) captures the cyclone as it exits the loop. The time gap between these two sets is around 36 hours. These two sequences of continuous cases offer a unique opportunity to study the complex steering flows.

## 2.2 Method

The steering flow was originally defined as an area-average barotropic wind around TC vortex (Chan and Gray, 1982). Here, the wind field retrieved from spaceborne SAR is at the sea surface level. Due to the friction, the steering flow speed is reduced at the surface level, but the direction is supposed to be similar to the steering flow in the free troposphere. Recently, Zhang et al. (2021) proposed a SHEW-2 (Surface Hurricane Estimates for Wind speed and Wind direction) model suggesting that the surface wind field is mainly composed by a symmetrical

vortex and a background wind vector (steering flow) at the surface level, which is validated by airborne observations and 130 SAR-derived wind fields.

Taking the advantages of three continuous cases within ~ 24 hours, this study proposed an original approach to determine complicated steering flows in three steps: 1) symmetric rotation winds, 2) a general steering flow over the three continuous cases synchronously, and 3) the remaining steering flow for each case by removing the general steering flow. Then, the surface wind vectors for the three continuous cases are as:

$$\begin{bmatrix} \overrightarrow{U_1}(r,\theta) \\ \overrightarrow{U_2}(r,\theta) \\ \overrightarrow{U_3}(r,\theta) \end{bmatrix} = \vec{V}_g + \begin{cases} \overrightarrow{U_{m1}}(r) + \vec{V}_{s1} \\ \overrightarrow{U_{m2}}(r) + \vec{V}_{s2} \\ \overrightarrow{U_{m3}}(r) + \vec{V}_{s3} \end{cases} \quad (1)$$

Where $(r,\theta)$ are the distance and angle in a Polar Coordinate System respectively, $\overrightarrow{U_i}$ (*i*=1,2,3) is the reconstructed wind vector for three cases respectively, $\overrightarrow{U_{mi}}(r)$ is used to represent the rotation wind vectors for the axisymmetric vortex for *i*th (*i*=1,2,3) case, $\vec{V}_g$ is the general steering flow over the three cases, and $\vec{V}_{si}$ is the remaining steering flow for *i*th (*i*=1,2,3) case. In the second step, the rest steering flow is set as zero ($\vec{V}_{si} = 0$). By fitting the three reconstructed wind speeds of $\overrightarrow{U_i}$ (*i*=1,2,3) to the three SAR winds synchronously, the general steering flow ($\vec{V}_g$) is determined. With the determined general steering flow, each case is fitted to the SAR-wind respectively, and the rest steering flow ($\vec{V}_{si}$) is determined respectively.

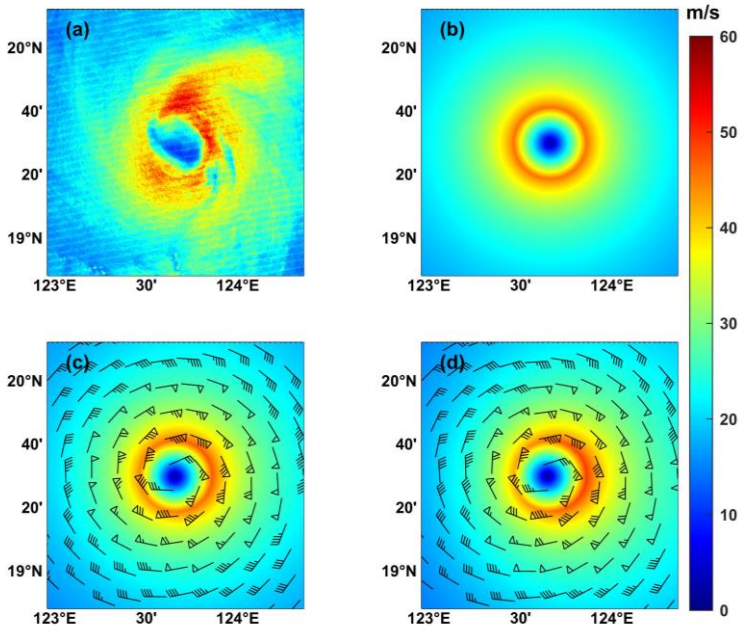


Fig. 2. Method of steering flow determinations: (a) SAR-derived sea surface winds for the first case acquired at 09:53 UTC on August 25, (b) extracted symmetrical vortex, (c) general steering flow fitted to three cases synchronously, and (d) remaining steering flow after removing the unified steering flow.

Taking the first case as an example, by fitting to the SAR-derived winds (Fig. 2a) acquired at 09:53 UTC on August 25, the best-fitted symmetrical wind field ($\overrightarrow{U_{m1}}$) as shown in Fig. 2b is determined associated with the center location, maximum winds and the radius of maximum wind (RMW). Then, the best-fitted general steering flow ($\vec{V}_g$) is determined over three cases, and the reconstructed wind field ($\vec{V}_g + \overrightarrow{U_{m1}}$) is shown in Fig. 2c. Then, we fit the respective rest steering flow to each case one by one by removing the general steering flow and the final reconstructed wind field ($\overrightarrow{U_1} = \vec{V}_g + \overrightarrow{U_{m1}} + \vec{V}_{s1}$) is shown in Fig. 2d. The fitting processes for the other five SAR-winds are demonstrated in Fig. A2 to Fig. A6. And the details of SHEW-2 model fitting have been presented in Zhang et al. (2021).

## 3 Steering flows from SAR-Winds

We determine the steering flows for Typhoon Saola (2023) by using the new method, thereby investigating the vortex movement during the loop track. The determined intensity ($U_{max0}$) and size indicated by RMW for the six cases and the steering flows are shown in Table I.

Table I TC vortex and two sets of steering flows

| Time (UTC) | | $U_{max0}$ (m/s) | RMW (km) | Steering flows | | | |
|---|---|---|---|---|---|---|---|
| | | | | $U_b$ (m/s) | | Direction | |
| 09:53 Aug-25 | within ~24 *hrs* | 45.7 | 20.83 | 1.5 | 2.1 | 151° | 194° |
| 21:46 Aug-25 | | 49.4 | 17.75 | | 2.2 | | 44° |
| 10:00 Aug-26 | | 60.9 | 17.31 | | 1.3 | | 322° |
| 21:31 Aug-27 | within ~24 *hrs* | 44.3 | 15.67 | 1.8 | 2.2 | 207° | 278° |
| 09:44 Aug-28 | | 60.9 | 9.90 | | 1.1 | | 35° |
| 21:37 Aug-28 | | 47.1 | 28.04 | | 0.9 | | 139° |

### 3.1 General Steering Flow and Summer Monsoon

Following our method (Section 2.2), we determine the steering flows: 1) the general steering flow over the three continuous cases within ~ 24 hours in red arrows and 2) the remaining steering flows in black arrows. The general steering in Fig. 3a for the first three continuous cases is the southeast summer monsoon from the Pacific Ocean, while the determined general steering flow in Fig. 3b is the southwest summer monsoon from the Indian Ocean (Ding & Chan, 2005; Xiang et al., 2013; He et al., 2024).

As shown in Fig. A1 from Xiang et al. (2013), two summer monsoon systems surround the loop track region in August: 1) southeast summer monsoon from the Pacific Ocean and 2) southwest summer monsoon from the Indian Ocean. Compared to Fig. 3c, the loop track is during two summer monsoon systems, and the determined general steering flows are consistent with the two summer monsoon systems there, respectively. As expected, the

summer monsoons are detected by using the general flow ($\vec{V}_g$ in Eq. 1), which makes it possible to removing the monsoon effects and determine the possible other steering flows.

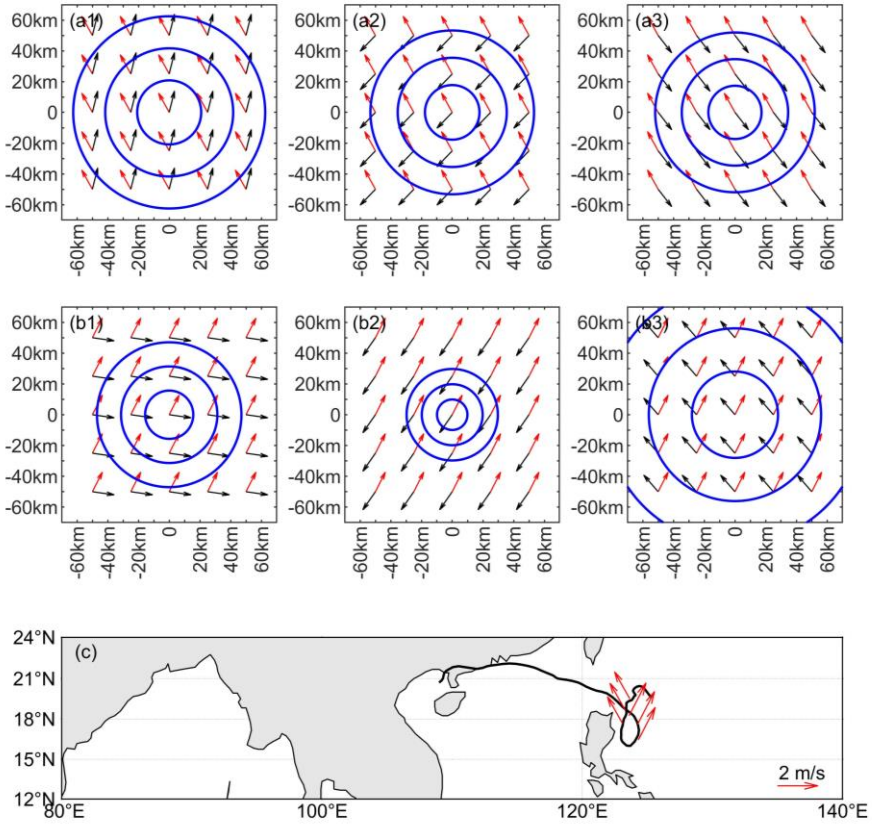


Fig. 3. Steering flows from (a) three continuous cases within ~ 24 hours from August 25 to 26, (b) three continuous cases within ~ 24 hours from August 27 to 28, and (c) the general steering flows from the above two sets results.

### 3.2 Remaining Steering Flows and Loop Track

As shown in Fig. 4, by removing the general steering flows determined from three consecutive cases (red arrows), the remaining steering flows over the SAR-derived surface wind field are determined and shown in black arrows. In the first case (Fig. 4a1), the black arrows indicate the southwest summer monsoon as the steering flow. In the second case (Fig. 4a2), the black arrows represent a steering flow that drives the vortex southwestward, initiating the loop track. As shown in Table I, the intensity of the southwestward steering flow is 2.2 m/s, while the general steering flow of monsoon is 1.5 m/s. The northeast steering flow in Fig. 4a2 then shifts to the northwest in Fig. 4a3. In the third case (Fig. 4a3), the northeast steering flow (1.3 m/s) in black arrows encounters the southeast summer monsoon (1.5 m/s), which would be the factor to cause TC Saola to move southward.

As shown in Fig. 4b1, the southwest summer monsoon (1.8 m/s) and the west steering flow shown in black arrows (2.2 m/s) make the vortex advance northeastward. As shown in Fig. 4b2, the steering flow in black (1.1 m/s) encounters the southwest summer monsoon, which blocks the vortex's way toward the east. As shown in Fig. 4b3, the black steering flow would be the southeast summer monsoon (0.9 m/s), and the loop track finished.

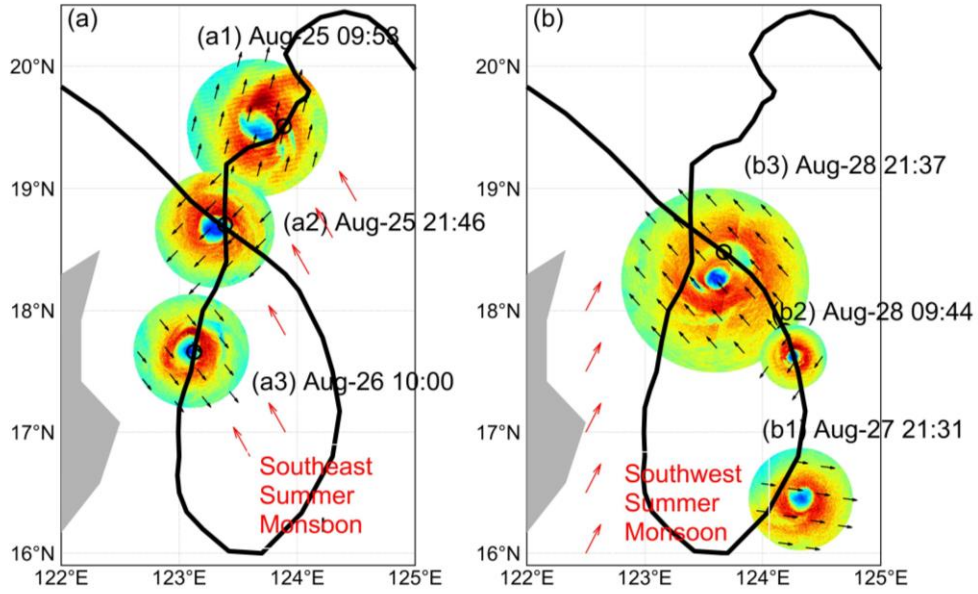


Fig. 4. Steering flows surrounding the loop track determined from: (a) three continuous cases from August 25 09:53 UTC to August 26 10:00 UTC, and (b) three continuous cases from August 27 21:31 UTC to August 28 21:37 UTC.

The steering flows determined by SAR observations surrounding the loop track are summarized as follows: 1) two summer monsoon systems from southwest and southeast, as shown by the two general steering flows in red arrows, and the rest steering flows in Fig. 4a1 and Fig. 4b3, 2) two steering flows from northeast (black arrows in Fig. 4a2 and Fig. 4b2) or northwest (black arrows in Fig. 4a3 and Fig. 4b1). Therefore, there would be at least one north (no matter from northeast or northwest) steering flow surrounding the loop area, which would be the factor to make the vortex advance southward and play an important role in the interesting movement of the loop track, associated with summer monsoon systems.

## 4 Summary

In this study, the loop track of Typhoon Saola (2023) is investigated by utilizing six SAR observations of a high-spatial-resolution wind field. We propose an original approach and find four steering flows: 1) southeast summer monsoon from the Pacific Ocean, 2) southwest summer monsoon from the Indian Ocean, and new steering flows from 3) northeast and/or 4) northwest.

Generally, this area in August is affected by both the western North Pacific summer monsoon (WNPSM) and Indian summer monsoon (ISM) (Ding & Chan, 2005; Xiang et al., 2013; He et al., 2024), which are detected by using the general flow ($\vec{V}_g$ in Eq. 1). The two summer monsoons are expected always there, but the loop track is not made by every TC passing this area. Therefore, if no new steering flows exsiting, the loop track cannot be made. Two new steering flow from northeast or northwest are determined by removing the monsoon effects as shown by the general steering flow over the three continuous cases, which can explain the TC movement during the loop track.

Although the footprint of steering flows on the surface wind field are not identical due to the friction, they can explain TC movement even during the complicated loop track of Saola. The size of Typhoon Saola (2023) is small, making the number modeling more difficult as the model grids in TC core area would be insufficient. As SAR TC observations increase timely, such as three RCM (RADARSAT Constellation Mission) satellites, the investigations of physic features, such as possible steering flows, would contribute to TC movement understanding and forecasting and surface wind reconstructions in storm surge modeling.

## Open Research

The SAR retrieved wind products were provided by NOAA (National Oceanic and Atmospheric Administration) STAR (Center for Satellite Applications and Research) and covered satellites of Sentinel-1 and RCM, (https://www.star.nesdis.noaa.gov/socd/mecb/sar/sarwinds_tropical.php). The best track data are from Schreck, Carl & National Center for Atmospheric Research Staff (Eds). "The Climate Data Guide: IBTrACS: Tropical cyclone best track data." Retrieved from https://climatedataguide.ucar.edu/climate- data/ibtracs-tropical-cyclone-best-track-data on.

## References

Chan, J. C. L., & Gray, W. M. (1982), Tropical Cyclone Movement and Surrounding Flow Relationships. *Mon. Wea. Rev*., 110, 1354–1374. doi:10.1175/1520-0493(1982)110<1354:TCMASF>2.0.CO;2.

Chan, J. C. L. (2005), The physics of tropical cyclone motion, *Annu. Rev. Fluid Mech.*, 37, 99–128. doi:10.1146/annurev.fluid.37.061903.175702.

Chu, P.-S., Kim, J.-H., & Chen, Y. R. (2012), Have steering flows in the western North Pacific and the South China Sea changed over the last 50 years?, *Geophys. Res. Lett.*, 39, L10704. doi:10.1029/2012GL051709.

Ding, Y., & Chan, J. C. L. (2005). The East Asian summer monsoon: An overview. *Meteorology and Atmospheric Physics*, 89(1–4), 117–142. doi:10.1007/s00703-005-0125-z

Hassanzadeh, P., Lee, CY., Nabizadeh, E. et al. (2020), Effects of climate change on the movement of future landfalling Texas tropical cyclones. Nat Commun 11, 3319. doi:10.1038/s41467-020-17130-7

He, L., Zhou, T., Guo, Z., Zuo, M., Ren, Z., Chen, X., et al. (2024), Northward extension of East Asian summer monsoon since the Miocene set by the uplift of Tibetan Plateau. *Geophys. Res. Lett.*, 51, e2023GL107262. doi:10.1029/2023GL107262

Howell, B., Egan, S., and Fine, C., (2022): Application of microwave space-based environmental monitoring (SBEM) data for operational tropical cyclone intensity estimation at the Joint Typhoon Warning Center. *Bull. Amer. Meteor. Soc.*, 103(10), E2315-E2322, doi:10.1175/BAMS-D-21-0180.1.

Klotz, B. W., & Jiang, H. (2016), Global composites of surface wind speeds in tropical cyclones based on a 12 year scatterometer database, *Geophys. Res. Lett.*, 43. doi:10.1002/2016GL071066.

Kossin, J.P. (2018), A global slowdown of tropical-cyclone translation speed, *Nature*, 558, 104–107. doi:10.1038/s41586-018-0158-3.

Lin, N., & Chavas, D. (2012), On hurricane parametric wind and applications in storm surge modeling, *J. Geophys. Res.*, 117, D09120. doi:10.1029/2011JD017126.

Marsooli, R., Lin, N., Emanuel, K. et al. (2019), Climate change exacerbates hurricane flood hazards along US Atlantic and Gulf Coasts in spatially varying patterns. *Nat. Commun.*, 10, 3785. doi:10.1038/s41467-019-11755-z

Reul, N., Chapron, B., Zabolotskikh, E., Donlon, C., Mouche, A., Tenerelli, J., ... and Kudryavtsev, V., (2017), A new generation of tropical cyclone size measurements from space, *Bull. Amer. Meteor. Soc.*, 98(11), 2367-2385. doi:10.1175/BAMS-D-15-00291.1.

Wang, S., & Toumi, R. (2021), Recent migration of tropical cyclones toward coasts, *Science*, 371(6528), 514–517. doi:10.1126/science.abb9038

Xiang, B., B. Wang, W. Yu, and S. Xu (2013), How can anomalous western North Pacific Subtropical High intensify in late summer?, *Geophys. Res. Lett.*, 40, 2349–2354, doi:10.1002/grl.50431.

Zhang, G., Perrie, W., Li, X., & Zhang, J. A. (2017). A hurricane morphology and sea surface wind vector estimation model based on C-band cross-polarization SAR imagery. IEEE Transactions on Geoscience and Remote Sensing, 55(3), 1743–1751. doi:10.1109/TGRS.2016.2631663

Zhang, G., & Perrie, W. (2018), Effects of asymmetric secondary eyewall on tropical cyclone evolution in Hurricane Ike (2008), *Geophys. Res. Lett.*, 45(3), 1676–1683. doi:10.1002/2017GL076988

Zhang, G., Li, X., Perrie, W., & Zhang, J. A. (2021), Tropical cyclone winds and inflow angle asymmetry from SAR imagery. *Geophys. Res. Lett.*, 48(20), e2021GL095699. doi:10.1029/2021GL095699.